COLDEX: A TOOL TO STUDY COLD SURFACES IN ACCELERATORS

V. Baglin
CERN, Geneva, Switzerland

Abstract

With the advent of more and more accelerator machines based on superconducting technology, the detailed understanding of the cryogenic vacuum system is of primary importance for the design and operation of modern machines. COLDEX was built to study the beam / cold surfaces interactions in LHC in the context of the electron cloud build-up. This paper reviews the main results obtained with COLDEX for Cu, the LHC material and a-C coating the proposed anti-multipacting surface for the LHC upgrade. It presents also recent results obtained with a laser treated surface, a potential anti-multipacting material for the next generation of colliders operating at cryogenic temperature.

INTRODUCTION

In the last decades, there have been an increasing number of projects or studies, which are based on the use of superconducting technologies. Thus, unless and anti-cryostat is included in the design, the associated vacuum system shall operate at cryogenic temperature. This is the case of superconducting RF cavities and superconducting magnets installed in synchrotrons or linacs and storage rings. Some examples of built machines are the Hadron Electron Ring Accelerator (HERA) and the European X-Ray Free ELectron Laser facility (XFEL) both at Desy, the Tevatron at Fermilab, the Relativistic Heavy Ion Collider (RHIC) at Brookhaven, the Large Hadron Collider (LHC) at CERN and the synchrotron SIS-100 of the Facility for Antiproton and Ion Research (FAIR) at Darmstadt. Examples of past or future projects are the Superconducting Super Collider (SSC), the International Linear Collider (ILC), the Future Circular hadron-hadron Collider (FCC-hh) and the Super Proton Proton Collider (SPPC).

When operating with cryogenic machines, the molecules can be physisorbed or condensed on the vacuum chamber wall. In some circumstances, these molecules are therefore available for subsequent desorption in the gas phase, leading to potential limitation of the machine operation.

The LHC is one of the first superconducting storage ring which operation can be potentially limited by the desorption of molecules from the cryogenic beam tube [1]. For this reason, the LHC arc vacuum system is made of a cold bore into which is inserted a perforated beam screen to control the gas density level [2]. The molecules desorbed from the beam screen under synchrotron radiation and beam induced electron cloud bombardments, can either be physisorbed on the 5-20 K beam screen surface or pumped through the beam screen's holes towards the 1,9 K cold bore which almost acts as a perfect sink for all gases except He. The detailed understanding of the beam interaction, via synchrotron radiation and beam induced electron cloud, with this innovative concept of perforated beam screen / cold bore vacuum system was of primary importance for the success of the LHC project.

The COLD bore EXperiment (COLDEX), was built, in collaboration with the NIKHEF institute of Amsterdam, to study the interaction of the synchrotron radiation with an LHC type vacuum system. After 2 years of construction, the cryostat was delivered at CERN by Nov. 1997 and, following commissioning, installed in the Synchrotron Light Facility 92 of the Electron Positron Accumulator (EPA) in Feb. 1998 during the Large Electron Positon (LEP) collider shutdown [3]. Until Apr. 2001, 69 runs were performed at EPA out of which 11 were conducted with the COLDEX cryostat installed in the accumulator where e^- and e^+ beams circulated through a 2.2 m long Cu beam screen with 1 % transparency and 70 mm inner diameter. The remaining studies were performed with the cryostat removed from within the accumulator and installed on a tangential synchrotron radiation beam line. In this way, it was possible to irradiate COLDEX with synchrotron radiation of 45 and 194 eV critical energies, in the range of the LHC machine. Unperforated and perforated, stainless steel, Cu, Cu-colaminated on stainless steel and cryosorbers equipped beam screens were deeply characterised under synchrotron radiation for the detailed design of the LHC machine. Irradiations were performed at 11 mrad grazing incidence on a 2.2 m long beams screens of 50 mm inner diameter with, when applicable, 1 % transparency [4, 5, 6, 7]. Specific studies using gas injections to characterise the beam screen equipped with cryosorbers were then conducted till Dec. 2001 [7].

Later, the COLDEX cryostat was installed during the 2002 shutdown in a bypass system of the SPS ring in BA4. An intense study campaign with perforated Cu beam screens started with the SPS scrubbing week of June 2003. In the context of the "electron cloud crash program", until Nov. 2004, 11 runs with LHC type beams using different beam structures, intensities and with several surface conditions were performed in 18 months before the LHC ring installation [8, 9, 10, 11, 12]!

In 2014, after the successful operation of the beam screen for the LHC exploitation, the cryostat was refurbished to house an amorphous carbon (a-C) coated Cu beam screen to study the proposed design for the LHC upgrade, the High-Luminosity LHC (HL-LHC) [13, 14, 15, 16]. For 2 years, 6 dedicated machine developments periods were held to study the a-C coating at cryogenic temperature which was already proven to be an efficient back-up to beam conditioning for the electron cloud mitigation of the room temperature SPS ring [17].

With the recent development of new technologies to mitigate the electron cloud build and their potential implication for the HL-LHC or Future Circular Colliders, a laser treated beam screen was installed for first tests in 2017 [18].

This paper gives an overview of the main results obtained with the COLDEX system when used to study the electron cloud interaction with Cu, a-C coated, and laser treated surfaces. Details discussions, available for the interested reader, are given in the references.

EXPERIMENTAL

The COLDEX cryostat is mounted in a bypass of the SPS ring, located in BA4. When in "OUT" position, the beams circulate through a standard SPS vacuum chamber. During the studies, the system is placed in IN position where the proton beams circulate through the 2.8 m long cryostat, as shown in Figure 1. The system can move, within one hour from one position to another, while the cryostat is held at cryogenic temperature. Due to the reduced beam pipe aperture, the extraction kickers, towards the LHC injection tunnel, TI8, are interlocked with the "IN" position. Two sector valves placed upstream and downstream to the cryostat, define the vacuum sector 41737, which decouples the cryogenic vacuum sector from the SPS ring. This decoupling allows to cool down and warm up the cryostat without perturbing the routine operation of the machine.

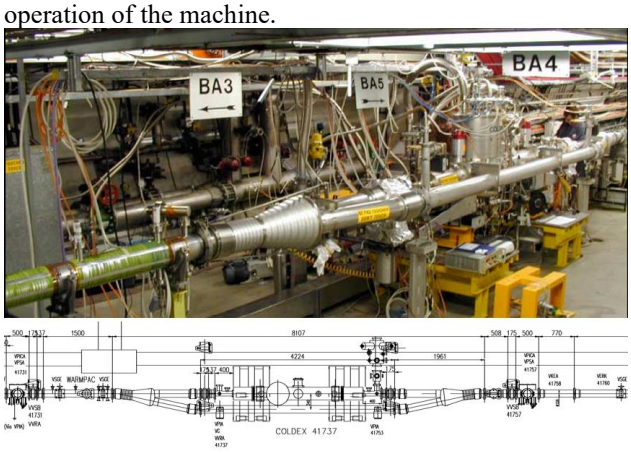

Figure 1: Top, picture of the device and, bottom, layout of the COLDEX cryostat installed in the bypass of the SPS ring.

As shown in Figure 2, many instruments are used with the COLDEX cryostat to monitor the interaction of the proton beam with the tested surface. The total and partial pressure are recorded along the system with calibrated instruments: a Bayard-Alpert gauge and a residual gas analyser (BA and RGA respectively). Measurement ports are provided upstream, downstream and in the middle of the cryostat. Electrodes are placed along the beam screen to collect charges, signatures of the beam-vacuum system interactions. The beam induced heat load is measured with additional room temperature calorimeters, WArm MultiPAC calorimeters, WAMPAC, and with the temperature increase along the cold beam screen [19]. The WAMPAC is made of a liner inserted into the vacuum pipe. From the measurement difference between the liner temperature and its surrounding tube, ΔT, the beam induced heat load, $\dot{Q}$, dissipated onto it can be derived in dynamic and steady state conditions using equations (1) and (2) respectively.

$$\dot{Q} = C\frac{\mathrm{d}\Delta T_{Eq}}{dt} \quad (1)$$

Where C is the thermal capacity of the liner.

$$\dot{Q} = \frac{\Delta T_{Eq}}{R} \quad (2)$$

Where R is the thermal resistivity and ΔT_{Eq} the temperature difference, at equilibrium, between the liner and its surrounding tube.

The WAMPAC is calibrated by applying a known heat, in an insulated cable welded along the liner, to measure the thermal parameters, C and R.

In COLDEX, the heat load on the beam screen, $\dot{Q}_{BS}$ is derived from the enthalpy (h_{He}), difference of the gaseous helium between the downstream and upstream beam screen temperatures and the He mass flow measurement, $\dot{m}$, see equation (3).

$$\dot{Q}_{BS} = \dot{m}\left[h_{He}(T_{down}) - h_{He}(T_{up})\right]C\frac{\mathrm{d}\Delta T_{Eq}}{dt} \quad (3)$$

Using an insulated powered cable stretched along the beam screen, the measurement system could be cross calibrated by applying a known heat load and the detection limit was estimated to be ~ 100 mW/m.

A gas injection system is used to dose the beam screen surface with known quantities of gas while monitoring the pressure drop of a calibrated volume with a capacitance gauge. By changing the pressure over the helium bath, the cold bore temperature is controlled from the lambda point (2.17 K) until 5 K. The bore can operate also in a "warm mode" from 200 to 300 K. The beam screen temperature is controlled using gaseous helium from 10 to 120 K. In static mode, a controlled helium flow along the beam screen maintains a temperature difference across the extremities from 2 to 10 K. Solenoids are placed at the cryostat extremity to supress the beam induced multipacting in these areas.

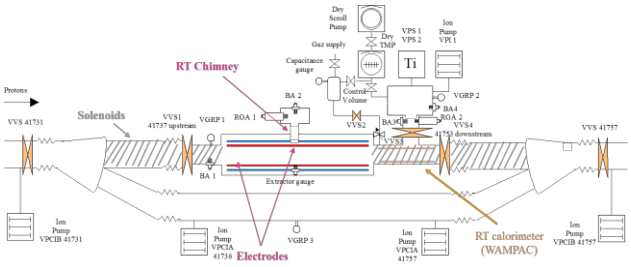

Figure 2: Schematic of the COLDEX bypass.

One of the difficulties to evaluate the pressure in a cryogenic vacuum system is due to the potential re-adsorption on the cold surface of the desorbed molecules before their detection by the vacuum instruments. Another limitation is due to the possible detection by the instruments of the molecules desorbed from the external parts of the cold beam screen. For this reason, the axial conductance shall be minimised and the beam screen long enough to ensure that the pressure rise observed at the central part is only due to the interaction of the beam with the beam screen surface. Moreover, the production of holes along a beam screen with optimised dimensions, similar to the ones used in this study, reduces to zero the impact on the vacuum measurements of these end effects. A chimney, held at room temperature, placed as close as ~ 1 mm to the beam screen's middle port, collected all the molecules from the cryogenic system for their detection with Bayard-Alpert (BA) vacuum gauge BA2 and residual gas analyser (RGA) 1. Figure 3 shows, on the left, a picture of the beam screen central part, and, on the right the Cu chimney during its introduction. A stainless-steel grid is placed at the beam screen's middle port to allow the passage of the image current and to avoid the development of high order modes in the chimney volume.

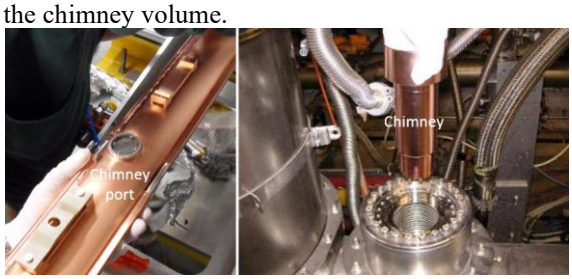

Figure 3: Left, central part of the beam screen, right, Cu chimney. Courtesy of R. Salemme.

The direct detection of electrons presence is of primary importance to support the observation of electron cloud formation. For this purpose, two electrodes are used in COLDEX, one located at the beam screen extremity and one located in the chimney, as shown in Figure 4. The beam screen electrode is located behind the beam screen holes at ~ 20 cm from the beam screen extremity and the chimney electrode is placed behind the beam screen grid (Figure 3), in the middle of the cryostat. These electrodes can be biased from – 1kV to + 1 kV with a detection limit of 0.1 nA.

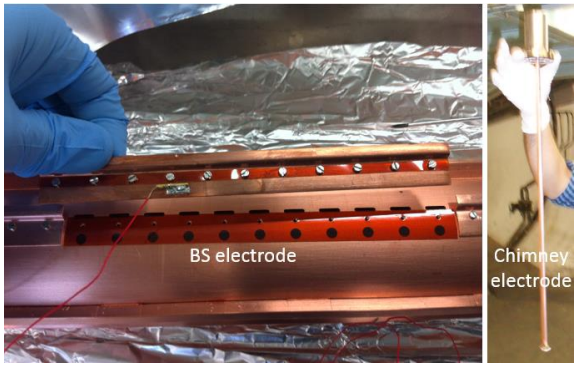

Figure 4: Left, beam screen electrode, right, chimney electrode. Courtesy of R. Salemme.

The impedance of the whole set up was optimised to guarantee a negligible contribution of it to the total heat load measured by the beam screen [11, 12]. The beam screen's aperture continuity is ensured by cold to warm transitions, see Figure 5. The design is very similar to the LHC one. It uses a Cu plated stainless steel to minimise the beam power loss and heat load onto the beam screen. A thermal anchoring to the COLDEX thermal screen, held at ~ 90 K, was produced to define the temperature gradient along the transition. A set of RF fingers, placed externally and at each extremity of the transition, allow the passage of the image current along the vacuum chamber pipe. Tapers are used to adjust the shape of the beam screen to its surrounding pipes.

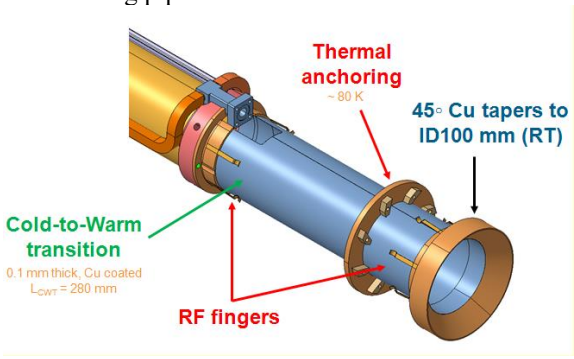

Figure 5: The COLDEX cold to warm circular transition.

Opposite to the LHC, which is a storage ring which collide proton beams at 7 TeV, the SPS ring is used to accelerate beams for end users such as fix target experiments or for the LHC injection. For this reason, during a SPS cycle of ~ 20-30 s, the proton beam is injected at 26 GeV in several batches from the PS and may be accelerated to 450 GeV before being extracted.

Table 1 shows the main SPS parameters and compares them with the LHC nominal parameters. During the studies described below, the typical proton bunch population was in the range of 10^{11} with a spacing of 25 ns between bunches, both parameters being strictly equal to the LHC ones.

However, the SPS beam energy (thus the beam emittance) is much lower than in the LHC and it is limited

to 450 GeV. Moreover, the SPS filling factor is restrained to 31 % for impedance reasons. A direct extrapolation of the results presented below to the LHC, relies therefore on some assumptions. For example, neglecting the impact of the beam emittance and the filling factor on the observed phenomena, an estimate of the LHC heat load can be done by multiplying the measured heat load by the COLDEX apparatus by the ratio of the respective filling factors (×0.79/0.31 for 4 SPS batches). On the other hand, the results presented here can still be used as inputs to simulation codes for extrapolation to other cryogenic machines.

Table 1: LHC & SPS machine parameters.

Parameters	LHC	SPS	
Beam energy (GeV)	7 000	26	450
Bunch length (ns)	1	2.8	1.7
Revolution period (μs)	89	23	
Batch spacing (ns)	-	225	
Beam current (mA)	560	55/110/165/220	
Number of batches	-	1/2/3/4	
Number of bunches	2808	72/144/216/288	
Filling factor (%)	79	9/16/24/31	
Bunch current (proton/bunch)	$1.1\ 10^{11}$		
Bunch spacing (ns)	25		

COPPER SURFACE

The interaction of an electron cloud with copper, the surface material of the LHC arcs, was studied from May 2002 until November 2004.

Two types of beam screens were produced, an oval-shape beam screen with H84-V66 dimensions [8, 11] was used the first year to gain experience with the SPS beams and a circular beam screen (ID67) was then used [9, 10, 12]. Both beam screens with 1% transparency were made of OFE copper. In the first version, the perforations were made of 2 × 73 circular holes of 7 mm diameter located in the horizontal plane. In the second version, the perforations were made of 2 × 131 rounded slots. The slots were 2 mm wide and 7.5 mm long. An electron shield to protect the cold bore from unwanted heat load towards the cold bore was placed behind each slot (see Figure 4).

Electron cloud signatures

The observation of electron cloud with the COLDEX set-up was confirmed by pressure & heat load increase concomitant with electron detection.

A bunch intensity scan with 4 SPS batches was done with the beam screen held at 12 K and the cold bore at 3 K. Figure 6 shows the heat load measured on the 12 K beam screen as a function of the bunch population. The curve has a threshold at $7\ 10^{10}$ proton/bunch above which the heat load increases linearly with the bunch population. Such behaviour is a typical signature of the electron cloud formation.

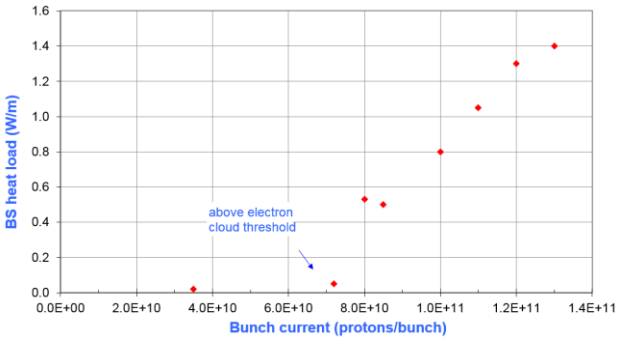

Figure 6: Electron cloud induced heat load vs bunch intensity for the circular Cu beam screen held at 12 K.

As shown in Table 2, in agreement with the observation of an electron cloud when increasing the bunch spacing from 25 ns to 75 ns, the electron current measured by the chimney electrode and the heat load on the beam screen are strongly reduced by ~ a factor 10. Other values measured at the beam screen and chimney electrodes for different configurations and conditioning are discussed in detail in Ref. [20].

Table 2: Electron cloud activity and heat load for 25 and 75 ns bunch spacing.

Bunch spacing (ns)	Electron cloud activity (μA)	Heat load (W/m)
75	1.6	0.2
25	20	1.4

Long-term behaviour

The long-term behaviour could be observed during dedicated SPS scrubbing which lasted typically 1-2 weeks. Figure 7 and Figure 8 are showing the evolution of the heat load on the beam screen due to beam induced electron cloud and the partial pressure evolution.

To avoid the scattering due to different filling factor inherent to a scrubbing period, the data of Figure 7 were normalised to 4 batches of SPS. Following beam conditioning to 12 A.h, and an estimated electron dose of 20 mC/mm^2, the final heat load was ~ 1.5 W/m [9]. According to simulations performed for WAMPAC 3, a Cu calorimeter with the same circular geometry as the COLDEX beam screen, the corresponding maximum secondary electron yield was estimated to be ~ 1.3 in agreement with a scrubbed surface [21].

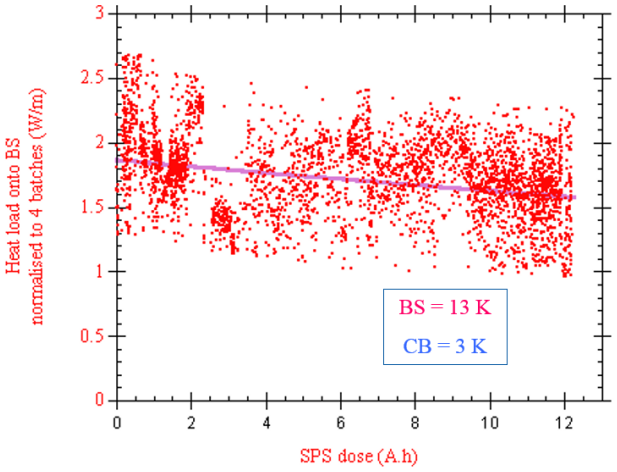

Figure 7: Heat load on the circular beam screen due to beam induced electron cloud [9].

In the presence of an electron cloud, the vacuum chamber wall is subjected to electron bombardment. Although the pumping speed of a cryogenic system held in the range 5-20 K, like LHC, can be very large (several thousand litre per sec per meter of beam tube), the electron irradiation stimulates the molecular desorption of tightly bound molecules.

Of primary importance for superconducting machines, is the hydrogen desorption. Indeed, as shown in Figure 8, the desorbed hydrogen can be physisorbed and accumulated on the beam screen surface at 8 K leading to a pressure increase due to the subsequent recycling of the weakly bounded hydrogen. This phenomenon is the LHC beam screen perforation raison d'être. As shown in Figure 8, the hydrogen partial pressure levels off after 1 h thanks to the beam screen's slots through which hydrogen can be pumped on the cold bore, and then decrease following beam conditioning. The hydrogen desorption yield was estimated to be ~ 5×10^{-2} H_2/e.

The electron bombardment stimulated also the desorption of other molecular species. However, their pressure level is two order of magnitude lower than hydrogen indicating a much lower recycling capability. For this reason, only the sum of the primary desorption, η, and recycling desorption, η', over the sticking coefficient, σ, was measured. The measured values range from 2×10^{-2} to 2×10^{-1} molecules/e.

It must be stressed that longer electron bombardment results to a surface conditioning associated with the reduction of the desorption yield for all gases as shown in [9] and observed for LHC which has a vacuum life time much larger than 100 h despite the presence of an electron cloud in the arcs [22].

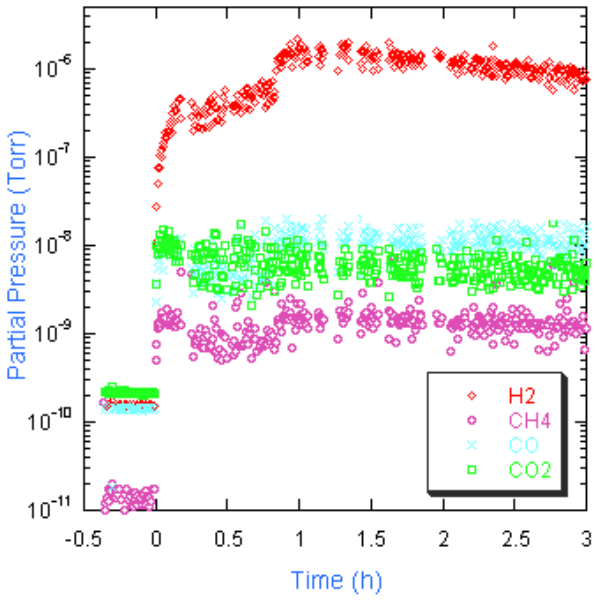

Figure 8: Partial pressure evolution during electron cloud irradiation of the oval beam screen held at 8 K with a cold bore at 4.2K [8].

Effects on pressure of physisorbed and condensed gases

As shown above, the accumulation of molecules on the cryogenic surface may lead to molecular recycling. In a real machine, gas molecules may accumulate at specific location during cool down or temperature excursion and accumulate during beam operation under electron cloud bombardment triggering pressure transients after modification of the beam parameters such as bunch intensity, filling scheme etc. [23].

Hence, several studies were performed with H_2, CO and CO_2 to investigate the interplay and the impact on the LHC design of the gas physisorption and condensation. To do so, with the extremity valves closed and the cold bore temperature held above 100 K, a known quantity of gas was injected into the system after which the beam screen temperature was increased to maintain a pressure level along the beam screen length in the range of 10^{-5} mbar. This method allowed the molecules to be uniformly distributed on the beam screen thanks to the very large impingement rate. The temperature was then slowly set back to below 15 K to allow gas cryosorption and finally the cold bore cooled down to 3 K.

Figure 9 shows the hydrogen recycling under electron cloud bombardment for 10^{15} H_2/cm^2 condensed on the beam screen held at 5 K. A large pressure increases up to 6×10^{-8} Torr followed by a fast decrease is seen. The derived recycling yield, η'/σ, equals 3 H_2/e. This large yield provokes a fast flushing of the hydrogen molecules trough the holes towards the cold bore. Thus, the pressure remains for a very short time (0.005 A.h) above the 100 h life time limit of LHC (~ 10^{-8} Torr for H_2). However, during this

process, no significant heat load increase on the beam screen (larger than 0.1 W/m) as compared to the bare surface was observed.

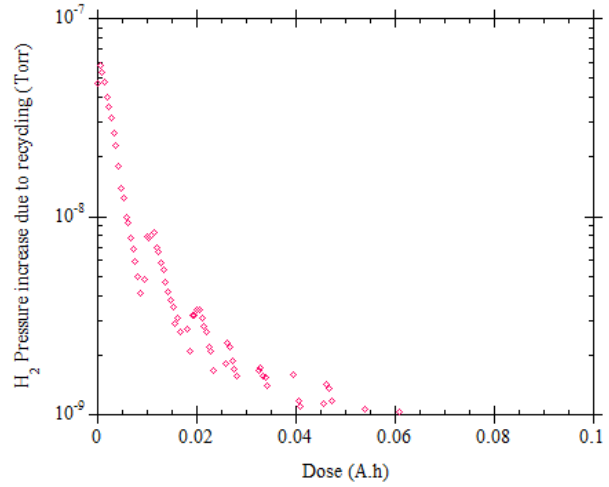

Figure 9: Hydrogen recycling under electron cloud irradiation when two SPS batches circulated with 10^{15} H_2/cm^2 condensed on the beam screen [10].

Figure 10 shows the result of a similar experiment with carbon monoxide recycling under electron cloud bombardment when 5×10^{15} CO/cm^2 are condensed on the beam screen held at 5 K. A pressure increases up to 1.5×10^{-8} mbar followed by a slow flushing of the CO molecules towards the cold bore is observed. The computed recycling yield, η'/σ, equals 0.4 CO/e. This value is much lower than for hydrogen, thereby the CO partial pressure remained above the 100 h life time limit for LHC (~ 10^{-9} Torr of CO) for a much longer period of at least 0.5 A.h. In this case also, the heat load increase on the beam screen associated with the amount of condensed gas was negligible.

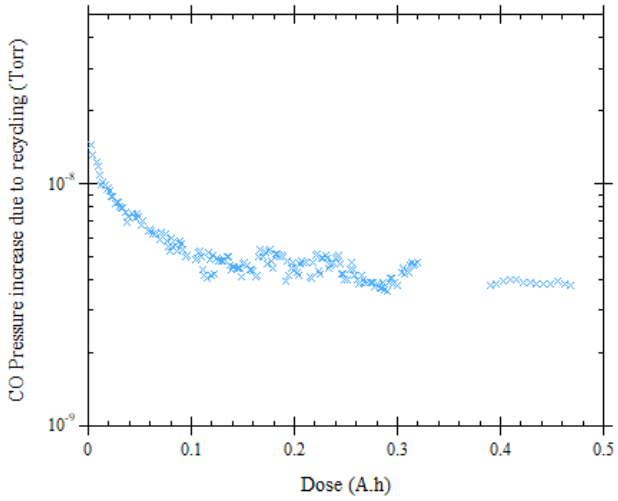

Figure 10: Carbon monoxide recycling under electron cloud irradiation when one SPS batches circulated with 5 10^{15} CO/cm^2 condensed on the beam screen [10].

The condensation of 15×10^{15} CO_2/cm^2 on the beam screen held at 15 K revealed a similar behaviour as carbon monoxide. However, as shown in Figure 11, the carbon dioxide molecule was cracked into carbon monoxide and oxygen under the electron bombardment: the resulting partial pressure of CO was seven times the partial pressure of CO_2. A slow flushing of the molecules towards the cold bore was observed with a computed recycling yield, η'/σ, of 0.01 CO_2/e. Again, for 1 circulating batch, the pressure increases remained above the 100 h life time limit of LHC for several hours with a negligible heat load increase.

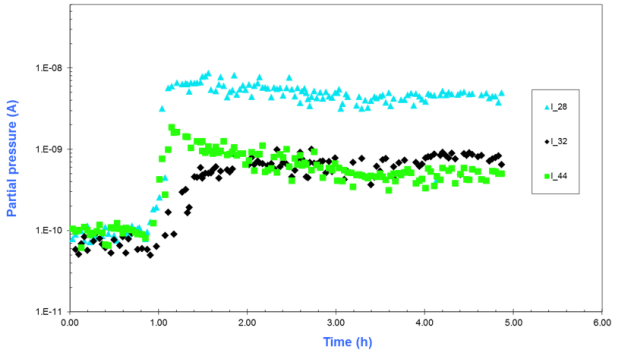

Figure 11: Carbon dioxide recycling and dissociation under electron cloud irradiation.

Impact of thick layers of condensates

In the event of the condensation of thick layers of gas, after *e.g.* a redistribution of molecules from the cold bore to the beam screen following a magnet quench, the impact on the machine operation may be dramatic as anticipated in [23]. A very similar scenario was unfortunately recently observed with the LHC following a probable air inlet in one interconnect of the 16L2 half-cell [24, 25].

Figure 12 shows the heat load induced by the electron cloud when 60×10^{15} CO/cm^2 is condensed on the beam screen. Due to the modification of the surface's secondary electron yield by the condensate, the observed heat load increased above 5 W/m for a long period. In the meantime, the hydrogen and carbon monoxide partial pressures reached 10^{-6} and 10^{-7} Torr respectively.

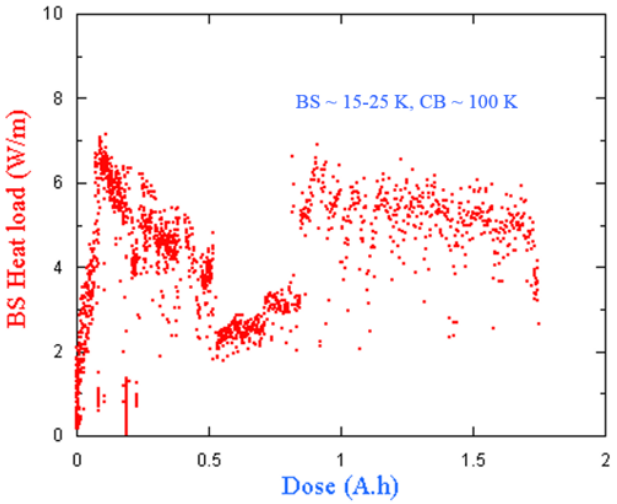

Figure 12: Beam screen heat load when 1, 2, 3 and 4 batches circulated with 60 10^{15} CO/cm^2 condensed on the beam screen [10].

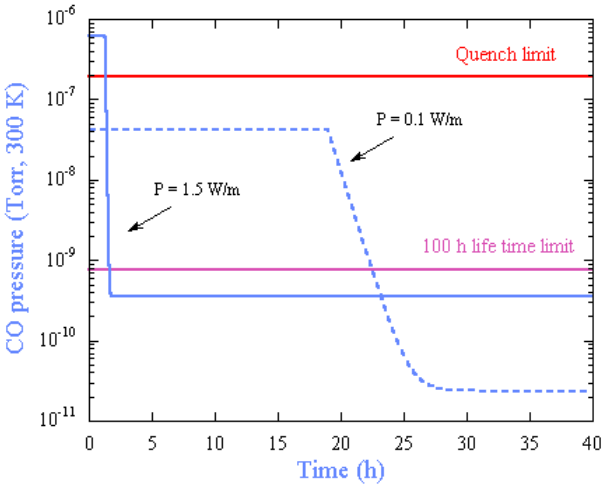

Figure 13: Vacuum transient due to the condensation of 25 10^{15} CO/cm^2 on the beam screen [10, 23].

Thus, the condensation of many monolayers of gas can be harmful for the operation of a superconducting machine. Figure 13 shows the computed carbon monoxide partial pressure using desorption yield data measured in the laboratory [26]. The curves are calculated for two values of heat load dissipated on the beam screen.

As shown, for 25×10^{15} CO/cm^2 condensed on the LHC beam screen, in the presence of electron cloud, the CO partial pressure is well above the 100 h life time limit. The lower the electron cloud activity, the longer the time is required to flush the carbon monoxide molecules from the beam screen to the cold bore. Several hours of beam circulation are needed at a low electron cloud activity (P = 0.1 W/m)

The removal of the carbon monoxide molecules can be speeded up by increasing the electron cloud activity. However, a too large electron cloud activity will stimulate a too high pressure level which may ultimately lead to a magnet quench. This is the case when 1.5 W/m is dissipated on the beam screen by the electron cloud.

To mitigate the above effect, beam screen heaters were integrated into the LHC design. Without beam operation, the heaters allows to warm up the beam screen above 80 K while maintaining the cold bore below 4.5 K, thereby flushing most of the gases towards the cold bore, with the exception of the water molecules [2].

At cryogenic temperature, although there is no thermal desorption of water, the H_2O desorption can be stimulated by electron bombardment. This is the case of unbaked surfaces or surfaces previously exposed to humidity. For this reason, it is recommended to pump down as long as possible an unbaked beam pipe before its cooling down to evacuate the maximum of water from the pipe. To do so, 5 weeks of pump down are required in the LHC machine before cooling.

Figure 14 shows the total pressure and the beam screen heat load for 2×72 circulating bunches. In the first part of the study, the pressure decreased by one order of magnitude until 10^{-5} Pa (10^{-7} Torr), conversely, the heat load increase up to 8 W/m while the beam screen temperature was drifting from 8 to 20 K due to the large beam induced heat loads! At t=100h, the beam screen was warmed up to 240 K while keeping the cold bore at 120 K with the beam circulating for a couple of hours during which a further vacuum conditioning was observed. A t=150h, the beam screen and cold bore were once again cooled down to 10 and 4.2 K respectively. The pressure continued to decrease further by one order of magnitude while the measured heat load on the beam screen was ~ 0.5-1 W/m.

Clearly, the temperature excursion up to 240 K together with the beam circulation contributed to the strong reduction of the heat load. Previous studies have shown that condensed water modifies the secondary electron yield of a surface. Indeed, a maximum secondary electron yield as large as 2.3 was measured in the laboratory with 150 monolayers [27]. Since water is desorbed from a Cu beam screen above 200 K, the origin of the previously described heat load is attributed to the water condensation. Indeed, before the experiment, the extremities of the experimental system were baked while the beam screen was kept at room temperature. Although the thermally desorbed gas was evacuated by the turbomolecular pumping, some molecules, in particular water, were sorbed on the beam screen. In the LHC, this undesirable situation

is avoided by adding a sector valve at each cold to warm transition to decouple the room temperature vacuum system from the cryogenic temperature vacuum system.

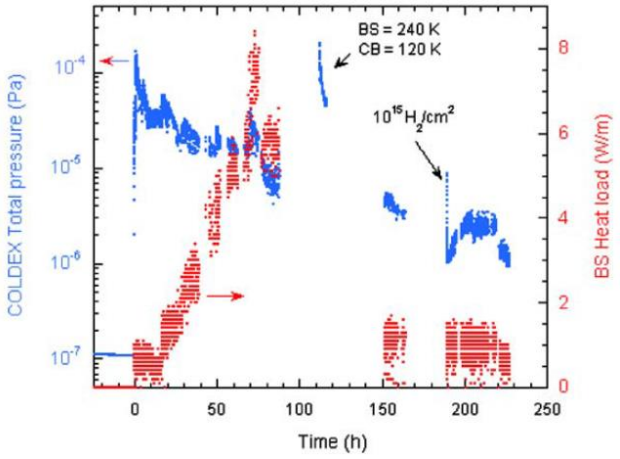

Figure 14: Total pressure and heat load on the beam screen for 2x72 circulating bunches of 0.8 – 1.1 10^{11} protons/bunch [8].

Other observations

In the presence of electron cloud, the heat load measured on the beam screen held at cryogenic temperature was compared to the heat load measured on a room temperature Cu pipe using the WAMPAC located upstream to COLDEX [19]. As expected, both equipment showed the same results indicating that both secondary electron yield were the same for both systems irrespective of their operating temperature [9, 22]. Obviously, as shown above, the presence of physisorbed and condensed gas may modify the secondary electron yield of the cryogenic surface leading to difference between heat loads measured at cryogenic and room temperature.

Several experiments were led to investigate further the behaviour of a cryogenic system in the presence of electron cloud and its impact on operation:

1. The COLDEX was kept under vacuum (P ~ 10^{-8} Torr) at RT for 2 months. After cooling down, no significant increase of the total pressure nor the heat load was noticed.
2. Similar observations were also made when, while held at RT, COLDEX was vented to air and pumped back before cooling down.
3. Finally, the COLDEX was kept to atmospheric pressure for 2 weeks and pumped down to 10^{-4} Torr before valving off the turbomolecular pump. Then, the beam screen was cooled down to 10 K and finally the cold bore to 3 K. This protocol gave the same observations as above.

CARBON COATED SURFACE

Since 2010, CERN is preparing the LHC upgrade: the High-Luminosity LHC (HL-LHC), a project which was approved by the CERN council in June 2016. This project consists in multiplying by 5 the LHC luminosity with an objective of 3 000 fb^{-1} accumulated in the mid 2030ies which corresponds to the production of more than 1 million Higgs bosons! [13].

For this purpose, the optics and the LHC matching section are modified by an entire production of new final focussing quadrupole magnets around ATLAS and CMS experiments. Table 2 shows the LHC and HL-LHC main parameters. The reduction of the normalised emittance and the doubling of the bunch population will be obtained after Long Shutdown 2 following the LHC Injector Upgrade (LIU) program [17]. The installation of the new focussing magnets and the deployment of the upgraded matching section will allow, after Long Shutdown 3, in the 2nd semester of 2026, to start a new era for the LHC employing the full capability of the Achromatic Telescopic Squeeze optic to further reduce the beam size at the collision point thereby increasing further the luminosity.

The expected high luminosity will be levelled to ~ 5×10^{34} Hz/cm^2 in order to maintain, at an acceptable level for the experimental detectors, the number of collisions at the interaction point. Although the detector experiments encapsulated as much as possible the collision point, a large amount of the produced debris will escape from the collision point towards the focussing superconducting quadrupoles. For this reason, the HL-LHC beam screen is shielded with tungsten, on its external side, to protect the cold mass from premature ageing ensuring the desired life time for the superconducting magnets [28, 13].

In order to mitigate electron multipacting thereby reducing the heat load on the cryogenic system and the background to the experiments, a-C coating, of the inner beam screen side, is proposed as a second major upgrade of the LHC-like beam screen design. This technology was recently successfully deployed for the CERN SPS machine to mitigate electron cloud [29]. Indeed, this coating acts as an anti-multipactor since the maximum secondary electron yield measured in the laboratory equals 1+/- 0.1 at a primary electron energy of 200 eV [30]. However, this coating was never evaluated at cryogenic temperature. For this reason, the COLDEX experiment was refurbished and equipped with a a-C coated (~ 400 nm thick) beam screen as shown in Figure 15 [14].

Table 3: LHC and HL-LHC beam parameters.

Parameters	LHC		HL-LHC
	Nominal	Ultimate	Nominal
Energy (TeV)	7		
Luminosity (x10^{34} Hz/cm^2)	1.0	2.3	5*
Current (mA)	584	860	1090
Proton per bunch (x10^{11})	1.15	1.7	2.2
Number of bunches	2808		2736
Bunch spacing (ns)	25		
Minimum β* (m)	0.55		0.15
Normalised emittance (μm)	3.75		2.5

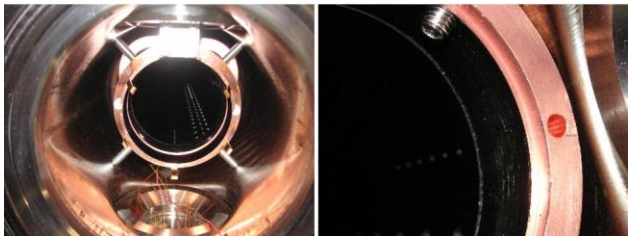

Figure 15: Picture of COLDEX extremity with a-C coated beam screen. Courtesy of B. Jenninger.

For 2 years, several important studies were conducted without and with protons beams [31]. The first observation was the demonstration of the large porosity of the ~ 400 nm thick coating. Indeed, at cryogenic temperature, the cryosorption capacity of hydrogen, measured with an adsorption isotherm, was estimated to be larger than 2×10^{17} H_2/cm^2 below 10 K *i.e.* more than 100 time the Cu capacity! A second observation, linked to the molecular capacity of the coating, was the thermal desorption of molecules at high temperature. Low coverage of hydrogen desorbs until ~ 60 K whereas other gases desorbed above 80 K.

Therefore, the working operating temperature of the HL-LHC beam screen needs to be studied in detail in a specific experimental set-up equipped with a 500 nm thick a-C coated sample to identify an acceptable temperature window [32]. Table 4 shows a compilation of the obtained results for the main gas species in the temperature range of interest for the HL-LHC inner triplets. As said above, in the 40-60 K temperature range, hydrogen is thermally desorbed for any surface coverage. Therefore, any temperature variation of the HL-LHC beam screen may lead to unwanted pressure oscillations thereby provoking beam induced background to the experiment or magnet quench in the ultimate case of very large pressure excursion. For this reason, and for this type of coating, an acceptable temperature range would be 60-80 K in which no hydrogen is physisorbed, thereby not available for desorption. In this temperature range, the other gases are available for desorption only when condensed in large quantities thus after several month of beam operation. An appropriate warm up at regular intervals will then suffice to guarantee a low enough surface coverage [33].

Table 4: Temperature range of desorption peaks from a 500 nm thick a-C coating [33].

T	H_2	CH_4	CO	CO_2
40-60 K	Any coverage	$> 10^{17}$ CH_4/cm^2	$> 2\times10^{16}$ CO/cm^2	$> 10^{18}$ CO_2/cm^2
60-80 K	No coverage	$> 5\times10^{16}$ CH_4/cm^2	$> 5\times10^{15}$ CO/cm^2	$> 10^{17}$ CO_2/cm^2

Long term operation of the SPS beams during scrubbing runs, with an accumulated beam dose till 10 A.h, were conducted to study the interaction of the LHC-like proton beam (4×72 bunches, 25 ns, up to 1.5×10^{11} protons/bunch) with the a-C coating held at cryogenic temperature. The studied beam screen temperatures were at 10, 50 and 80 K with the cold bore held at 3 - 4.5 K. No pressure rise larger than a few 10^{-10} mbar, no significant heat load larger than 0.2 W/m (opposed to 1.5 W/m for Cu, as shown in Figure **7**) and no significant current on the central electron pick-up larger than 0.1 nA (opposed to a few µA for Cu, see Table 2) were observed. Unfortunately, the beam screen electrode was not available during the a-C coating qualification phase.

The impact of operating temperature and gas absorption were studied during dedicated machine development periods. Hydrogen was condensed on the beam screen with 3×10^{16} H_2/cm^2 and studied at 10, 15, 20, 25 and 50 K. Carbon monoxide was condensed on the beam screen with 2×10^{16} CO/cm^2 and studied at 10 and 50 K. Finally, carbon dioxide was condensed on the beam screen with 3×10^{16} CO_2/cm^2 and studied at 10 and 60 K with the cold bore held, in all cases, at 3 – 4.5 K. Similar to the long term studies of a bare surface, no dynamic pressure attributed to the electron stimulated desorption larger than 10^{-9} mbar, nor electron multipacting activity above 0.1 nA were observed. The measured dynamic heat load was 0.2 +/- 0.1 W/m in all cases.

Given the difficulty to trigger and observe a signature signal of electron cloud, in complement to the standard calibration of the instruments, a specific protocol was developed to assess the detection limit of the electron probes. Using the pumping and desorption properties of the a-C coating, the temperature of the beam screen was increased up to 60 K during the beam circulation. Around 40-60 K, the natural hydrogen thermal desorption, lead to an escalation of the beam gas ionisation modifying the collection current at the chimney electrode [31]. Figure 16 shows a superposition of three plots with: top, the SPS beam intensity, middle, the pressure at the COLDEX extremities (VG1, VG3) and COLDEX centre (VG2) and bottom, the electron current measured at the COLDEX chimney located at the same position as VG2. The hydrogen thermal desorption, up to 5×10^{-8} mbar, induced by the beam screen temperature increase from 40 to 60 K, provoked a current read at the chimney electrode from 0.1 to 1.5 nA modulated by the passage of the SPS batches through the beam screen. This observation confirmed a detection limit of 0.1 nA for our electrode.

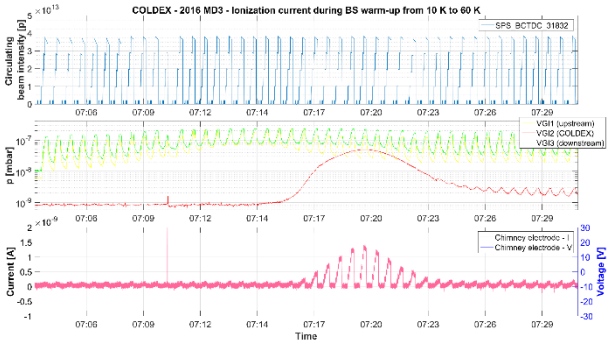

Figure 16: Top, SPS beam intensity, middle, total pressure along COLDEX, bottom, electron current at the COLDEX chimney, while increasing the a-C coated beam screen temperature from 10 to 60 K [31].

To assess the maximum secondary electron yield of the studied a-C coating, several PyCloud simulations were done. They demonstrated that the electron current detection was more sensitive than the heat load detection [15]. Figure 17 shows the simulation results using a model of the a-C secondary electron yield curve derived from laboratory measurements [31]. A maximum secondary electron yield of 1.1 can be derived from the electrical measurements (< 0.1 nA), in agreement with pressure and heat loads observations. This value is consistent with published a-C data [29] and recent measurement in the laboratory at cryogenic temperature [34].

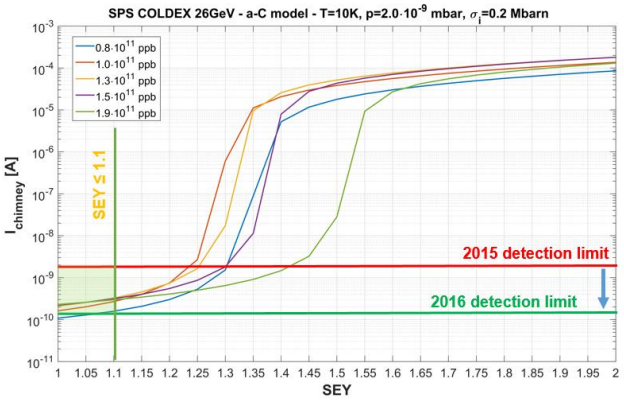

Figure 17: PyCloud simulation of the electron activity at the COLDEX chimney [31].

The above results confirmed the appropriate choice of a-C coating for the HL-LHC base line providing the coating is operated in appropriate conditions. Together with the use of the coating as an anti-multipactor technology the SPS upgrade [30] and its good behaviour in the LHC at room temperature [35], the technology will be deployed during the Long Shutdown 2 for a validation test in the LHC standalone magnets Q5R2, Q6R2, Q6L8 and Q5R8 during RUN3 before HL-LHC construction.

LASER TREATED SURFACE

Laser engineering surface were recently developed to lower the secondary electron yield of materials much below 1 [36, 37]. First studies at room temperature were successfully conducted in a short test section of the SPS showing results as good as a-C coating [38]. For this reason, with the objective to develop an alternative base line for the HL-LHC and to investigate the potential use with Future Circular Colliders, a laser treated beam screen was constructed for COLDEX [18].

Due to technological constraints, this laser treated beam screen was built out of 9 segments which were produced in collaboration with CERN – STFC and the University of Dundee, and finally assembled and tested at CERN, see Figure 18. The final beam screen was of the same dimensions as the ID 67 Cu and a-C coated beam screens.

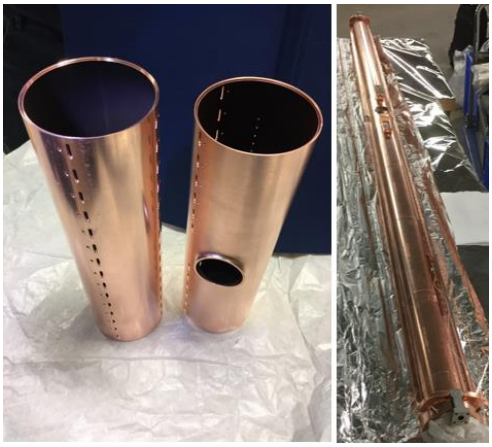

Figure 18: Left, segments of laser treated tube before their assembly at CERN, right assembled laser treated tubes to form a beam screen before its insertion into COLDEX [18].

Each segment was laser treated under nitrogen atmosphere at the University of Dundee with the following laser parameters: a wavelength of 532 nm (2.3 eV), a repetition rate of 200 kHz, a pulse length of < 15 ps, a focal spot diameter of 12 µm, an intensity of 0.4 TW/cm^2 (10^{30} ph/s/cm^2), a rotating speed of 10 mm/s and an advancing speed of 1-2 µm/s. The laser treatment lasted 3 days per segment. During the treatment, the laser head was fixed around which the ~ 25 cm long segment to be treated was rotating. Figure 19 shows the scanning electron microscope photography of a laser treated segment. The laser treatment produces groove, of 10 µm depth, located along the diameter of the segment and spaced by ~ 23 µm. A closer look to the surface shows a "cauliflower" like structure of ~ 3 µm size. X-ray Photoelectron Spectroscopy analysis indicates the presence of Cu and copper oxide, CuO, on the surface following the treatment. The maximum secondary electron yield measured in the laboratory is ~ 0.87 at a primary electron energy of 861 eV [38, 18]. As compared to standard Cu and a-C secondary electron yield curves, the curve of the laser treated surface has a maximum at much higher primary energies.

Therefore, the electron energy distribution resulting from interaction of the electron cloud with the surface will greatly differ from the interaction of the cloud with Cu or a-C surfaces.

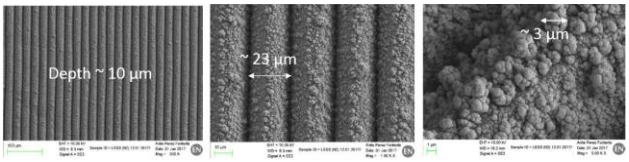

Figure 19: Scanning electron microscope photography of a laser treated beam screen segment. Courtesy A. Perez Fontenla, CERN EN-MME.

For 2 years, several studies were conducted without and with LHC-like beams, the main findings are summarised below. Detailed analysis and discussions will be published in a future report.

As shown in Figure 20, temperature programmed desorption (TPD) studies showed that H_2 is desorbed in the range 20-35 K, N_2 and CO in the range 20-40 K and CO_2 in the range 110-150 K. These values are strongly different from the one obtained with a-C coating and Cu surface underlying the fact that the TPD characterisation of materials is required to select the proper material for future applications [39].

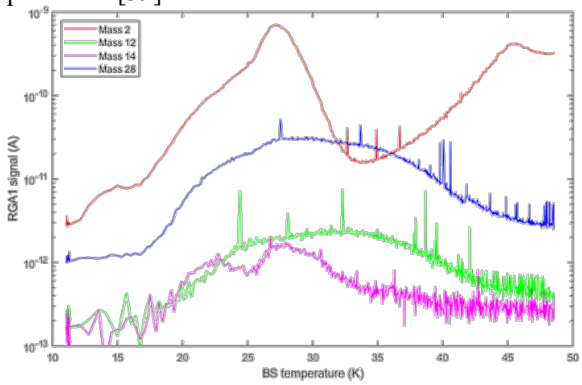

Figure 20: Temperature programmed desorption spectra from 10 to 50 K of the laser treated COLDEX beam screen. Courtesy of V. Badin.

Hydrogen transmission studies through the beam screen held at 20 K and the cold bore at 3 K, were also conducted showing the development of a pressure wave similar to the LHC case for He [40]. For a hydrogen flux of 2×10^{-3} mbar.ℓ/s, the measured speed of the H_2 wave was 12 cm/min and a pressure of 10^{-7} mbar at the beam screen centre. Of course, a lower hydrogen flux would reduce proportionally the wave speed and pressure level.

Six periods of 24 h were devoted to study the interaction of the LHC-like beam (4×72 bunches, 25 ns bunch spacing, 0.9 – 1.4 10^{11} proton/bunch, 26 GeV) with the laser treated surface.

With the COLDEX cold bore held at 3 K, the beam screen temperature was set at 10 and 50 K. At 10 K, no pressure rises larger than 10^{-10} mbar were observed in the centre of COLDEX although electron induced pressure rise in the 10^{-7} mbar range were present in the room temperature vacuum chambers upstream and downstream to COLDEX. At 50 K, the hydrogen was no pumped anymore by the laser treated beam screen and a pressure increase of ~ 10^{-9} mbar was noticed. When acting on the solenoids at the extremity, the pressure increase was slightly reduced, as expected, but not cancelled. This residual pressure increase may be attributed to the electron cloud generated in the COLDEX cold to warm transitions. Indeed, an electron current was measured on the beam screen electrode (0.1 µA for 50 V applied), whereas no electron signal was measured at the central chimney electrode.

Several studies were made with CO_2 condensed on the surface prior beam circulation. Although condensed quantities were as large as $1\div3\times10^{17}$ CO_2/cm^2, no pressure or beam induced heat load increases nor electron signals as compared to the bare surface situation were observed underlying the robustness of the material against gas condensation.

Specific studies with different beam structures were also performed to address the origin of the dynamic heat load observed with the laser treated surface. As shown in Figure 21, a dynamic heat load was measured in the warm laser treated calorimeter when the beam was dumped (ΔT = 0.3 K). When LHC-type beams circulated (4 batches with 1.3 10^{11} protons/bunch), this quantity amounts to ~ 80 mW/m opposed to 420 mW/m for the Cu surface. Although a signal was noticeable, the same quantity was barely measurable with enough accuracy for the laser treated beam screen held at cryogenic temperature. Operating the SPS with different bunch structure increasing the spacing from 200 ns to 2500 ns between batches or using 8b4e beams to supress the electron cloud build up indicated that the major part (if not all) of this heat load was due to the power losses attributed to the sample impedance. Indeed, beside the surface morphology of a laser treated surface which may affect its impedance, the present sample had grooves perpendicular to the beam path by construction which may further increase the power loss due to impedance.

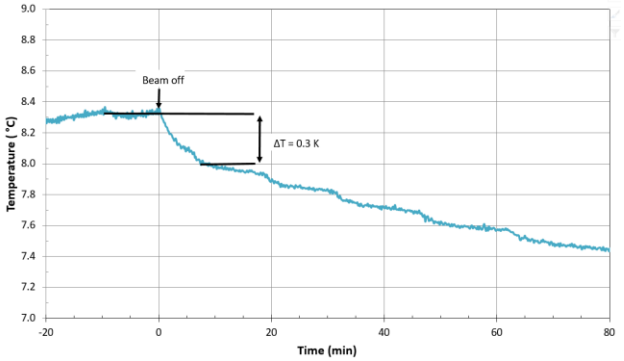

Figure 21: Observation of dynamic heat load at the warm laser treated calorimeter when LHC-type beams circulated. Courtesy B. Jenninger.

Finally, a specific run was held to study the behaviour of a laser treated beam screen in the presence of "large partial pressure". To this end, H_2 and N_2 were injected up to ~ 10^{-8} mbar inside the beam screen (held from 10 to 65 K) during beam circulation. Apart for the electron signal collected at the chimney electrode due to beam-gas ionisation (similar to Figure 16), no significant heat load increases were observed, demonstrating the robustness of the laser treatment in the presence of "large partial pressure".

CONCLUSIONS

The experimental modelling of cryogenic vacuum system is of paramount importance for the design and operation of superconducting machines.

For this reason, during the LHC design phase, the COLDEX experiment was installed in a bypass of the SPS ring to study the electron-cloud interaction with an LHC type beam screen. Data obtained with Cu material in laboratories could be then complemented by observations with beams on an LHC type mock-up. The studies confirmed the beam conditioning effect and the control of the gas density level by the beam screen perforation but highlighted the impact of the physisorbed and condensed gas on the machine operation leading to the setting-up of specific procedures for the LHC machine cool down and beam screen regeneration [2].

With the upgrade of the LHC machine, the HL-LHC, to be commissioned by mid-2026, the evaluation of the recently developed anti-multipacting surfaces such as a-C coating was needed [29, 13]. Qualifications at cryogenic temperatures with COLDEX showed no major showstopper for the use of a-C coating in superconducting machines, apart from a specific definition of the operating temperature owing to the material porosity [15, 16, 33]. These studies led to the pilot deployment of the a-C coating in four superconducting magnets of the LHC matching section for final validations during Run 3 before a full deployment during the HL-LHC construction phase.

A recently developed anti-multipacting surface such as laser treated beam screen was also evaluated at cryogenic temperature with COLDEX as an alternative to the a-C coating. The studies showed that this material has a very good behaviour and robustness against multipacting when LHC-type beams circulates. However, more detailed studies are still needed to assess the impact of the surface morphology on the beam performances together with studies at cryogenic temperature and room temperature evaluation in the LHC [35] before integrating such material in the HL-LHC vacuum system.

ACKNOWLEDGMENTS

I would like to warmly acknowledge the constant commitment and expertise of B. Jenninger during the design, installation(s) and operation of the COLDEX apparatus. I would like also to underline the skills of R. Salemme, the Beam Vacuum Operation section, in charge of the SPS vacuum operation, and the CRG group for their cryogenic expertise and support during the refurbishment and re-commissioning of the COLDEX system. Results with a-C coating and laser treated beam screens were mainly obtained by R. Salemme and V. Badin respectively, two fellows I had the pleasure to supervise during these studies. I am delighted to underline their ability to operate COLDEX and analyse the data. The a-C coating was successfully performed thanks to the talent of P. Costa Pinto. The laser treated beam screen fabrication, produced under the collaboration between CERN, STFC and the University of Dundee, was successfully coordinated by R. Salemme despite the tight schedule. I want to underline also the quality of the LHC-type beams delivered by the SPS operators and warmly acknowledge the HL-LHC project office and the TE department for their constant support during the a-C coating and the laser treated surface studies.

REFERENCES

[1] O. Gröbner. Overview of the LHC vacuum system. Vacuum 60 (2001) 25-34.

[2] The LHC design report. CERN-2004-003, CERN, Geneva, June 2004.

[3] J.P. Potier, L. Rinolfi. The LEP Pre-Injector as a multipurpose facility. Proc. of EPAC'98, Stockholm, Sweden, 22-26 June 1998.

[4] V. Baglin, I.R. Collins, C. Grünhagel, O. Gröbner and B. Jenninger. First from COLDEX applicable to the LHC cryogenic vacuum system. Proc. of EPAC'00, Vienna, Austria, 26-30 June 2000.

[5] V. Baglin, I.R. Collins, C. Grünhagel, O. Gröbner and B. Jenninger. Molecular desorption by synchrotron radiation and sticking coefficient at cryogenic temperatures for H_2, CH_4, CO and CO_2. Vacuum 67 (2002) 421-428.

[6] V. Baglin, I.R. Collins, C. Grünhagel, O. Gröbner and B. Jenninger. Synchrotron radiation studies of the LHC dipole beam screen with COLDEX. Proc. of EPAC'02, Paris, France, 3-7 June 2002.

[7] V. Baglin, I.R. Collins, C. Grünhagel, O. Gröbner and B. Jenninger. Cryosorbers studies for the LHC long straight section beam screens with COLDEX. Proc. of EPAC'02, Paris, France, 3-7 June 2002.

[8] V. Baglin, I.R. Collins, B. Jenninger. Performance of a cryogenic vacuum system (COLDEX) with an LHC type beam. Vacuum 73 (2004) 201-2016.

[9] V. Baglin, B. Jenninger. Pressure and heat load in a LHC type cryogenic vacuum system subjected to electron cloud. Proc. of ECLOUD'04, Napa, Ca, USA, April 2004.
[10] V. Baglin, B. Jenninger. Gas condensate onto a LHC type cryogenic vacuum system subjected to electron cloud. Proc. of EPAC'04, Lucerne, Switzerland, July 2004.
[11] B. Spataro et al. Impedances of the cold bore experiment, COLDEX, installed in the SPS machine. Nucl. Instr. And Meth. A 564 (2006) 38-43.
[12] B. Spataro et al. Coupling impedance studies and power loss measurement of the COLDEX upgraded vacuum chamber. Nucl. Instr. And Meth. A 581 (2007) 885-889.
[13] High Luminosity Large Hadron Collider (HL-LHC), Technical Design Report. CERN 2017-007-M, July 2017.
[14] R. Salemme, V. Baglin, F. Bellorini, G. Bregliozzi *et al.* Recommissioning of the COLDEX experiment at CERN. Proc. of IPAC 2015, Richmond, VA, USA, May 2015.
[15] R. Salemme, V. Baglin, G. Bregliozzi, P. Chiggiato. Amorphous carbon coatings at cryogenic temperatures with LHC type beams: first results with the COLDEX experiment. Proc. of IPAC 2015, Richmond, VA, USA, May 2015.
[16] R. Salemme, V. Baglin, G. Bregliozzi, P. Chiggiato. Vacuum performance of amorphous carbon coating at cryogenic temperature with presence of proton beams. Proc. of IPAC 2016, Busan, Korea, May 2016.
[17] LHC Injector Upgrade, Technical Design Report, CERN-ACC-2014-0337, CERN, Geneva, December 2014.
[18] R. Salemme, V. Baglin, S. Calatroni, P. Chiggiato *et al*. First beam test of laser engineered surface structures (LESS) at cryogenic temperature in CERN SPS accelerator. Proc. of IPAC 2018, Vancouver, Canada, May 2018. J. Phys.: Conf. Ser. **1067** 082017.
[19] V. Baglin, B. Jenninger. CERN SPS electron cloud heat load measurements and simulations. Phys. Rev. STAB, 6, 063201 (2003).
[20] V. Baglin, B. Jenninger. Preliminary results of June 2004 scrubbing run. Presented at the Accelerator Performance Committee, 18th June 2004.
[21] D. Schulte and F. Zimmermann. Electron cloud build up simulations using ECLOUD. Proc. of ECLOUD'04, Napa, Ca, USA, April 2004.
[22] V. Baglin. The LHC vacuum system: commissioning up to nominal luminosity. Vacuum 138 (2017) 112-119.
[23] V. Baglin. Vacuum transients during LHC operation. Proc. of LHC Project Workshop - Chamonix XIII, Chamonix, January 2004.
[24] J. M. Jimenez, S. Antipov, G. Arduini, A. Bertarelli, N. Biancacci *et al*. Observations, analysis and mitigation of recurrent LHC beam dumps caused by fast losses in arc half-cell 16L2. Proc. of IPAC 2018, Vancouver, Canada, 2018.
[25] B. Salvant, S. Antipov, G. Arduini, N. Biancacci, X. Buffat *et al*. Experimental characterisation of a fast instability linked to losses in the 16L2 cryogenic half-cell in the CERN LHC. Proc. of IPAC 2018, Vancouver, Canada, 2018.
[26] H. Tratnik, N. Hilleret, H. Störi. The desorption of condensed noble gases and gas mixtures from cryogenic surfaces. Vacuum 81 (2007) 731-737.
[27] V. Baglin, B. Henrist, N. Hilleret, E. Mercier, C. Scheurlein. Ingredients for the understanding and the simulation of multipacting. Proc. of the 10th Chamonix SPS&LEP performance workshop, Chamonix, January 2000.
[28] V. Baglin, A. Ballarino, F. Cerutti, R. Denz, P. Fessia et al. Conceptual design of the LHC interaction Upgrade – Phase – I. LHC Project Report 1163, Nov 2018.
[29] P. Costa Pinto, S. Calatroni, H. Neupert, D. Letant-Delrieux, P. Edwards *et al*. Carbon coatings with low secondary electron yield. Vacuum 98 (2013) 29-36.
[30] C. Yin Vallgreen, G. Arduini, J. Bauche, S. Calatroni, P. Chiggiato *et al*. Amorphous carbon coatings for the mitigation of electron cloud in the CERN Super Proton Synchrotron. Phys. Rev. ST Accel. Beams 14, 071001 (2011).
[31] R. Salemme. Space charge compensation and electron cloud effects in modern high intensity proton accelerator. PhD thesis, Universita di Roma Sapienza, October 2016.
[32] A.-L. Lamure, V. Baglin, P Chiggiato, B. Henrist. Adsorption/desorption from amorphous carbon coatings at cryogenic temperatures. Presented at AVS 64th International Symposium & Exhibition, Oct. 29 – Nov. 3, 2017, Tampa, FL, USA
[33] V. Baglin. Towards final validation of new temperature of BS triplets. Presented at the 8Th HL-LHC Collaboration Meeting, CERN, 15-18th October 2018.
[34] B. Henrist, V. Baglin, M. Haubner. Characterisation of technical surfaces at cryogenic temperature under electron bombardment. These proceedings.
[35] E. Buratin, V. Baglin, B. Henrist. Preliminary results obtained with the LHC Vacuum Pilot Sector. These proceedings.
[36] R. Valizadeh, O.B. Malyshev, S. Wang, S.A. Zolotovskaya, W.A. Gillespie, A. Abdolvand. Low secondary electron yield engineered surface for electron cloud mitigation. Appl. Phys. Lett. 105, 231605 (2014).
[37] R. Valizadeh, O.B. Malyshev, S. Wang, T. Sian, M.D. Cropper, N. Sykes. Reduction of secondary electron yield for E-cloud mitigation by laser ablation surface engineering. Appl. Surf. Sci. 404 (2017) 370-379.
[38] S. Calatroni, E. Garcia-Tabares Valdivieso, H. Neupert, V. Nistor *et al*. First accelerator test of

vacuum components with laser-engineered surfaces for electron cloud mitigation. Phys. Rev. Accel. Beams 20, 113201 (2017).
[39] V. Baglin, Ph. Lebrun, L. Tavian, R. van Weelderen. Cryogenic beam screens for high-energy particle accelerators. Proc. of ICEC24-ICMC2012, Fukuoka, Japan, 2012. CERN-ATS-2013-006.
[40] E. Wallen. Experimental test of the propagation of a He pressure front in a long, cryogenically cooled tube. J. Vac. Sci. & Technol. A15, 2949 (1997).